

Magnetization reversal and magnetic anisotropy in patterned Co/Pd multilayer thin films

Darren Smith,¹ Vishal Parekh,¹ Chunsheng E,¹ Shishan Zhang,² Wolfgang Donner,³ T. Randall Lee,⁴ Sakhrat Khizroev,⁵ and Dmitri Litvinov^{1,a)}

¹Department of Electrical and Computer Engineering, University of Houston, Houston, Texas 77204, USA

²Department of Chemical and Biomolecular Engineering, University of Houston, Houston, Texas 77204, USA

³Department of Physics, University of Houston, Houston, Texas 77204, USA

⁴Department of Chemistry, University of Houston, Houston, Texas 77204, USA

⁵Department of Electrical Engineering, University of California–Riverside, Riverside, California 92521, USA

(Received 6 September 2007; accepted 24 November 2007; published online 29 January 2008)

(Co/Pd)_N multilayers exhibit high vertical magnetic anisotropy and have been extensively explored as recording medium candidates for high density magnetic recording applications. In this work, (Co/Pd)_N multilayers are deposited by magnetron sputtering and patterned into large periodic arrays of 200 nm islands to enable controlled domain wall injection for quantitative comparison of magnetic anisotropy energies. Magnetic properties are correlated with x-ray photoelectron spectroscopy data, an approach commonly used to probe the binding energies and valence band positions. Confirming theoretical predictions, it is demonstrated that the degree of *d*-shell hybridization at Co/Pd interfaces directly correlated with the magnitude of magnetic anisotropy.

© 2008 American Institute of Physics. [DOI: 10.1063/1.2837049]

I. INTRODUCTION

(Co/Pd)_N multilayer films where thicknesses of cobalt and palladium layers are in a few monolayer range exhibit high magnetic anisotropy perpendicular to the film surface where variations of Co and Pd layer thicknesses in a bilayer stack have strong effect on multilayer magnetic properties.¹ Such magnetic multilayers have been extensively explored as recording medium candidates for high density magnetic recording applications.^{2,3} The origin of the perpendicular anisotropy is believed to be due to the hybridization of the *d*-shell electrons at the interfaces between Co and Pd layers.⁴

II. EXPERIMENTAL DETAILS

High anisotropy exchange coupled (Co/Pd)_N multilayers designed for bit-patterned medium applications were deposited using room temperature magnetron sputtering onto oxidized silicon substrates with a 5 nm Ta layer to promote exchange coupled films.⁵ Thicknesses of the Co and Pd layers are varied to modify the magnetic properties of the films as well as the deposition pressure. The multilayers were patterned into large arrays of 200 nm islands using ion beam proximity lithography described elsewhere.⁶ Magnetic properties of continuous and patterned multilayers were measured using magneto-optical Kerr effect (MOKE). X-ray photoelectron spectroscopy (XPS) was used to evaluate *d*-shell electron hybridization.

III. RESULTS AND DISCUSSION

Vertical *M*–*H* loops for a continuous and patterned (200 nm islands) (Co:3.2 Å/Pd:6.3 Å)₃₀ multilayer are shown in Fig. 1. Patterning results in a significant increase of the coercivity due to introduction of artificial domain wall pinning sites. Unlike domain wall nucleation and propagation in continuous films controlled by various defects and pinning sites, the bit geometry along with material parameters defines the domain wall nucleation fields in patterned films. The nucleation field, *H*_{*n*}, and the coercivity, *H*_{*c*}, of the patterned films are good indicators of magnetic anisotropy field, *H*_{*k*}, as long as the samples with the same island size are compared. Moreover, if the magnetization saturation, *M*_{*s*}, of the multilayer stays constant, *H*_{*n*} and *H*_{*c*} are equally good indicators of the magnitude of magnetic anisotropy, *K*_{*u*}.⁷

Vertical *M*–*H* loops for a set of continuous and patterned [CO(3 Å)/Pd(7 Å)]₃₀ multilayer films deposited at different pressures are shown in Fig. 2. The thicknesses of individual layers in the bilayer stack represent approximately

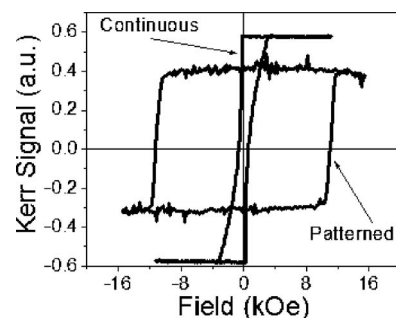


FIG. 1. Vertical *M*–*H* loops for continuous and patterned (Co:3 Å/Pd:7 Å)₃₀ multilayers.

^{a)}Author to whom correspondence should be addressed. Electronic mail: dlitvinov@uh.edu.

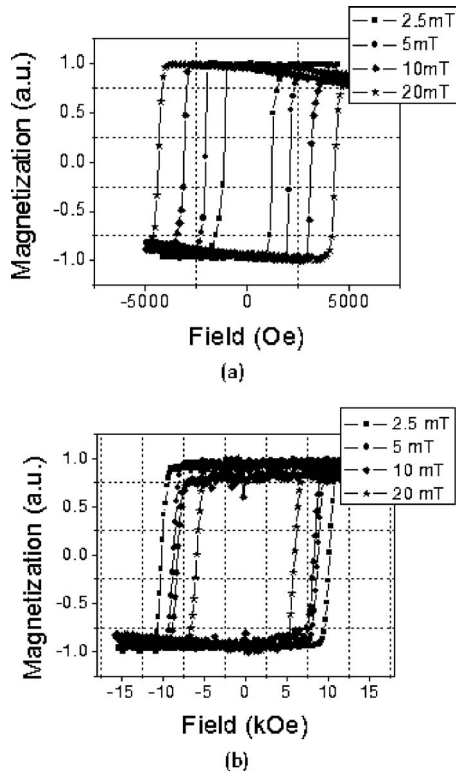


FIG. 2. Hysteresis loops for $[\text{Co}(3 \text{ \AA})/\text{Pd}(7 \text{ \AA})]_{30}$ films (a) before and (b) after lithographic patterning.

one and two monolayers for Co and Pd, respectively, and are the optimal thicknesses for highest perpendicular anisotropy. Although an increase in the coercivity is observed for increasing deposition pressures in the continuous films, the coercivity decreases after patterning as shown in Fig. 3. Significantly, all films had nearly identical magnetization saturation of 450 emu/cm^3 , thus indicating that stronger perpendicular anisotropy, K_u , is developed when the multilayers are deposited at lower pressure.

X-ray photoelectron spectroscopy (XPS), which is commonly used to probe the binding energies and valence band positions of materials, was used to analyze the multilayer films. Although the typical probing depth of XPS is limited to about 2–3 nm, it is sufficient for the evaluation of the one to two topmost bilayers in a multilayer stack and thus infer the relevant details of the band structure of the entire film. A

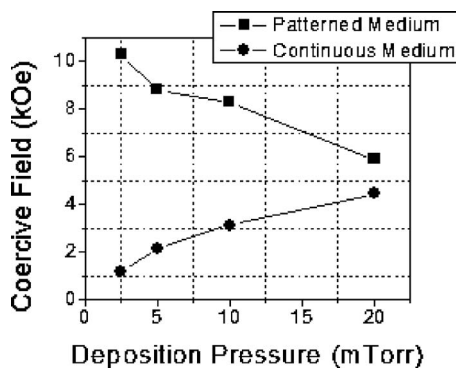


FIG. 3. Coercivity as a function of deposition pressure for continuous and patterned $[\text{Co}(3 \text{ \AA})/\text{Pd}(7 \text{ \AA})]_{30}$ multilayer films.

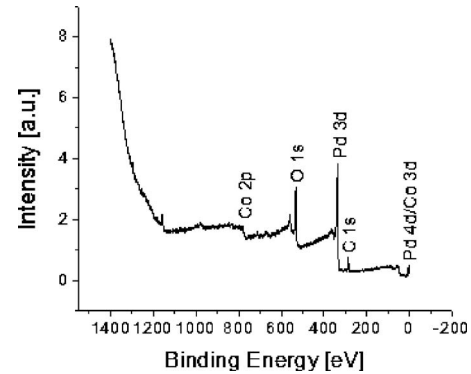


FIG. 4. An XPS survey scan for a $(\text{Co } 3 \text{ \AA}/\text{Pd } 7 \text{ \AA})_{30}$ multilayer studied in this work.

survey scan of a $(\text{Co/Pd})_{30}$ multilayer is shown in Fig. 4. The valence band data are located in the negative binding energy region where the Pd $4d$ and Co $3d$ electrons can be probed. The valence band peaks for pure Co and Pd samples are measured as 2.5 and 1.6 eV, respectively. The XPS spectra of $(\text{Co/Pd})_{30}$ are dominated by Pd signature, thus only the hybridization of Pd $4d$ electrons can be measured.

The valence position of the multilayers as a function of Co thickness for several deposition pressures is shown in Fig. 5. The decrease of the binding energy with the increasing Co thickness correlated with the observed decrease in magnetic anisotropy with the increasing Co thickness. Moreover, the binding energies for 20 mT samples are significantly closer to the valence position of pure Co than pure Pd, which is in agreement with the decrease in anisotropy field of the samples with increasing deposition pressure. Weaker hybridization of Pd atoms for samples with thicker Co layers and deposited at higher pressures results in lower anisotropy. Significantly, no measurable d -electron hybridization was observed for as-deposited CoPd alloys.

Pd atoms located further from the interface should experience less hybridization and hence less magnetic moment than the Pd atoms located immediately at the interface. XPS measurements will only yield an average for all of the layers within the probing depth of the material, so, if the additional Pd monolayers are not hybridized as strongly as those at the interface, we expect to see a drop in the valence position energy (closer to the position of pure Pd). Indeed, as the

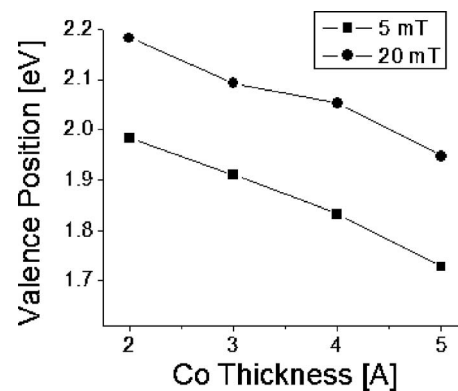


FIG. 5. Valence position of the $[\text{Co}(X)/\text{Pd}(7 \text{ \AA})]_{30}$ films sputtered at multiple deposition pressures.

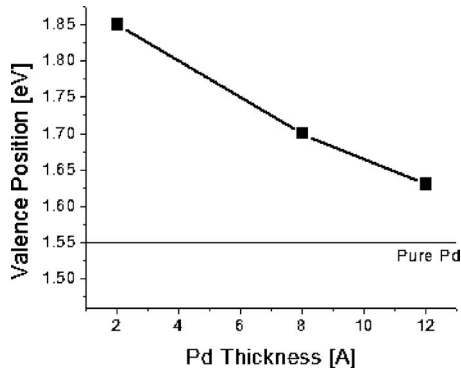


FIG. 6. Valence position of the $[\text{Co}(3 \text{ \AA})/\text{Pd}(X)]_{30}$ films sputtered at 2.5 mTorr.

thickness of the Pd layer in the multilayer structure increases, the valence position shifts toward the Pd baseline sample as shown in Fig. 6. This is in agreement with *ab initio* calculations⁸ that have shown that the Pd atoms nearest to the interface acquire a magnetic moment of $0.30 \mu_B$ due to *d*-electron hybridization, whereas the second layer from the interface has only $0.17 \mu_B$ and the third layer has $0.03 \mu_B$.

The dependence of the nucleation field values on the texture spread determined from the rocking curves is shown in Fig. 7. Lower deposition pressures result in better (111) textured films. While it has been reported that (111) texture may increase magnetic anisotropy,⁹ open questions remain regarding the role of crystallographic orientation in magnetic multilayers. The dependence of the nucleation field values in patterned multilayers on the average out-of-plane crystalline coherence length estimated using the Scherrer formula, $\langle L \rangle$

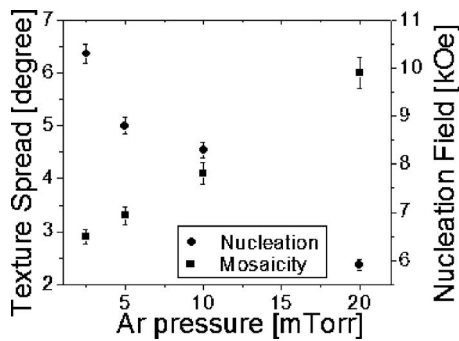


FIG. 7. Comparison of nucleation field values and film mosaicity for $[\text{Co}(3 \text{ \AA})/\text{Pd}(7 \text{ \AA})]_{30}$ films sputtered at different pressures.

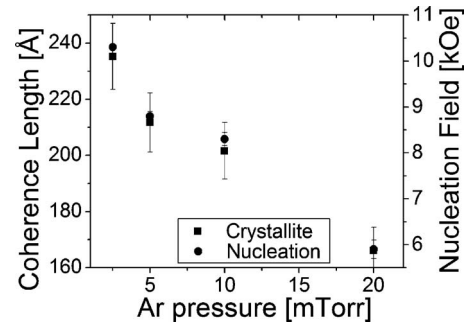


FIG. 8. Comparison of nucleation field values and crystalline coherence throughout the multilayer thickness for $[\text{Co}(3 \text{ \AA})/\text{Pd}(7 \text{ \AA})]_{30}$ films sputtered at different pressures.

$= K\lambda/B_{1/2} \cos \theta_B$, is shown in Fig. 8. Significantly, the Scherrer's length is smaller than the film thickness and indicates crystalline imperfections throughout the multilayer thickness. Similar to the effects of deposition pressure on film texture, lower deposition pressure results in better crystalline coherence throughout the multilayer thickness, which, in turn, results in higher magnetic anisotropy values.

IV. SUMMARY

In summary, magnetic properties of $(\text{Co}/\text{Pd})_N$ magnetic multilayers have been correlated with XPS data and, in turn, to the deposition conditions and structure thereof. It is found that samples with larger magnetic anisotropy exhibit strong shifts in the position of the Pd valence band, a signature of *d*-shell electron hybridization. It is also found that lower deposition pressure results in higher anisotropy films, which can be attributed to better crystallographic ordering and improved crystalline order throughout the multilayer thickness.

¹P. F. Garcia, D. Meinholdt, and A. Suna, *J. Magn. Magn. Mater.* **66**, 351 (1987).

²K. Ho, B. Lairson, Y. Kim, G. Noyes, and S. Su, *IEEE Trans. Magn.* **34**, 1854 (1998).

³T. Thomson, G. Hu, and B. Terris, *Phys. Rev. Lett.* **96**, 257204 (2006).

⁴G. A. Bertero and R. J. Sinclair, *J. Magn. Magn. Mater.* **134**, 173 (1994).

⁵Ch. E. D. Smith, S. Khizroev, D. Weller, J. Wolfe, and D. Litvinov, *J. Appl. Phys.* **98**, 024505 (2005).

⁶V. Parekh, Ch. E. D. Smith, A. Ruiz, P. Ruchhoeft, J. Wolfe, and D. Litvinov, *Nanotechnology* **17**, 2079 (2006).

⁷B. N. Engel, C. D. England, R. A. Vanleeuwen, M. H. Wiedmann, and C. M. Falco, *Phys. Rev. Lett.* **67**, 1910 (1991).

⁸M. Cinal and D. M. Edwards, *Phys. Rev. B* **55**, 3636 (1997).

⁹W. Peng, R. H. Vitoria, J. H. Judy, K. Gao, and J. M. Sivertsen, *J. Appl. Phys.* **87**, 6358 (2000).